Journal of Power Sources 211 (2012) 1–3

Contents lists available at SciVerse ScienceDirect

Journal of Power Sources

journal homepage: www.elsevier.com/locate/jpowsour

Short communication

Young's modulus of polycrystalline $Li_{12}Si_7$ using nanoindentation testing

J.B. Ratchford [a], B.A. Crawford [b], J. Wolfenstine [a], J.L. Allen [a], C.A. Lundgren [a,*]

[a] U.S. Army Research Laboratory, Adelphi Laboratory Center, 2800 Powder Mill Road, Adelphi, MD 20783, United States
[b] Nanomechanics Incorporated, Analytical Services Laboratory, 105 Meco Lane, Suite 100, Oak Ridge, TN 37830, United States

ARTICLE INFO

Article history:
Received 22 November 2011
Received in revised form
6 February 2012
Accepted 11 February 2012
Available online 19 February 2012

Keywords:
Lithium
Silicon
$Li_{12}Si_7$
Young's modulus

ABSTRACT

Young's modulus for $Li_{12}Si_7$ was determined from nanoindentation testing. Young's modulus for $Li_{12}Si_7$ was 52.0 ± 8.2 GPa. This value is in excellent agreement with estimated values of Young's modulus calculated from predicted values of bulk modulus using density functional theory.

Published by Elsevier B.V.

1. Introduction

The specific capacities of Li–Si alloys are four (1620 mAh g^{-1}, $Li_{12}Si_7$) to ten times (4200 mAh g^{-1}, $Li_{22}Si_5$) greater than graphite, making these alloys attractive alternatives to graphitic anodes in Li-ion batteries [1–5]. One problem with Li–Si alloys is that their capacities diminish with cycling as a result of substantial volume changes with Li-ion addition/removal which causes fracture and results in loss of particle contact. Another problem with Li–Si alloys that causes capacity fade is that it has been suggested that these alloys do not form a stable solid electrolyte interphase (SEI) layer. The SEI layer is continually being formed and destroyed [6,7]. In order to reduce capacity fade of Li–Si alloys knowledge of the mechanical properties of these alloys, like Young's modulus [8,9], is required. Young's moduli for Li–Si alloys were recently predicted by Shenoy et al. using density functional theory (DFT) calculations [8]. Ratchford et al. [10] measured Young's modulus for $Li_{22}Si_5$ using nanoindentation testing to verify the predicted value for $Li_{22}Si_5$ by Shenoy et al. [8]. The measured Young's modulus for $Li_{22}Si_5$ (35.4 ± 4.3 GPa) [10] was approximately one-half of the predicted value (~78 GPa) [8]. Ratchford et al. [10] showed that the disagreement between the measured and predicted values was not due to the testing procedure or microstructural variables of the alloy and concluded that the measured value represented the true property of this alloy [10]. Because of the disagreement between the measured and predicted values of Young's modulus for $Li_{22}Si_5$, more experimental measurements to verify the predicted mechanical properties of Li–Si alloys are needed. Therefore, the objective of this study was to measure Young's modulus for $Li_{12}Si_7$ using nanoindentation testing and compare the predicted value by Shenoy et al. [8] to this experimentally determined value.

2. Experimental

The same experimental methods that were used to synthesize, characterize and prepare samples of $Li_{22}Si_5$ for nanoindentation testing [10] were used for samples of $Li_{12}Si_7$. Therefore the experimental methods used for $Li_{12}Si_7$ are only briefly summarized in the following: X-ray diffraction was used to determine the phase purity of $Li_{12}Si_7$ from powder samples. Inductively coupled plasma-mass spectrometry (ICP-MS) was used to analyze the elemental composition of the synthesized $Li_{12}Si_7$. To prepare samples for nanoindentation, granules of $Li_{12}Si_7$ were cold mounted and polished to a mirror finish in mineral oil using standard metallographic techniques. The grain size of $Li_{12}Si_7$ was measured using the linear intercept method from optical images taken from the polished surface of samples etched in 0.2 wt.% water, 0.3 wt.% hydrochloric acid diluted with hexane. Young's modulus was determined from the load–displacement curve during unloading with nanoindentation using the Oliver–Pharr method [11,12]. Twenty tests were performed on the $Li_{12}Si_7$ samples. Standard reference materials of fused silica and tin were used to calibrate the instrument. All nanoindentation testing was performed under mineral oil.

* Corresponding author. Tel.: +1 301 394 2541; fax: +1 301 394 0273.
E-mail address: cynthia.a.lundgren2.civ@mail.mil (C.A. Lundgren).

0378-7753/$ – see front matter Published by Elsevier B.V.
doi:10.1016/j.jpowsour.2012.02.027

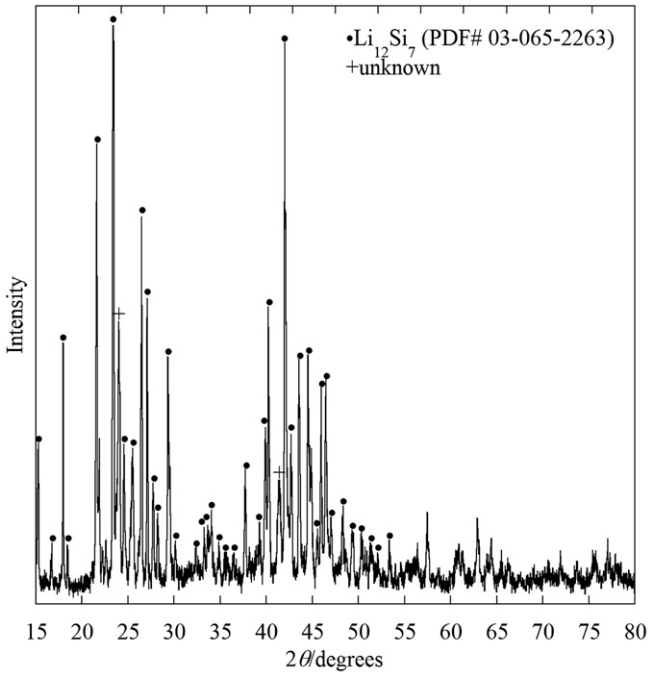

Fig. 1. X-ray diffraction pattern of the $Li_{12}Si_7$ alloy.

3. Results and discussion

The X-ray diffraction pattern for the $Li_{12}Si_7$ alloy is shown in Fig. 1. From the diffraction pattern it can be seen that the positions of the diffraction peaks are in good agreement with the positions of diffraction peaks in the International Centre of Diffraction Data's powder diffraction file for $Li_{12}Si_7$ (PDF# 00-040-0942). Impurity peaks corresponding to the (3 1 1) diffraction peak of Mo_4O_{11} (PDF# 01-089-6725) and the (1 1 1) diffraction peak of $MoSi_2$ (PDF# 01-081-0167) were observed in the pattern. The Mo originated from the crucible used to prepare the alloy. These results suggest that the material is predominately single phase $Li_{12}Si_7$ with Mo_4O_{11} and $MoSi_2$ impurities. The weight percentage of lithium in the $Li_{12}Si_7$ alloy obtained using ICP-MS was $28.6 \pm 1.5\%$. The expected weight percentage of lithium for the $Li_{12}Si_7$ alloy is 29.8% [13]. ICP-MS showed that the alloy was $1.8 \pm 0.5\%$ by mass molybdenum. In the worst case, the alloy is 2.3% by mass molybdenum. From this mass composition in conjunction with the densities of the impurities, the $Li_{12}Si_7$ alloy contains at most 0.4 vol.% $MoSi_2$ or 0.5 vol.% Mo_4O_{11}. Optical microscopy of the fine polished surface of a sample of the $Li_{12}Si_7$ alloy revealed no second phases and no porosity. Etching of this sample revealed that the grain structure is fairly equiaxed, with a grain size of 4 ± 1 μm.

Young's moduli for $Li_{12}Si_7$ and $Li_{22}Si_5$ [10] that were measured using nanoindentation are listed in Table 1. Table 1 shows that the average value of Young's modulus for $Li_{12}Si_7$ is 52.0 ± 8.2 GPa. In order to get an indication on the affect of the impurities on Young's modulus for the $Li_{12}Si_7$ alloy it was assumed that this measured value is that for a composite material composed of the alloy and

Table 1
Young's moduli of samples measured by nanoindentation.

Sample	E (GPa)
$Li_{12}Si_7$	52.0 ± 8.2
$Li_{22}Si_5$	35.4 ± 4.3

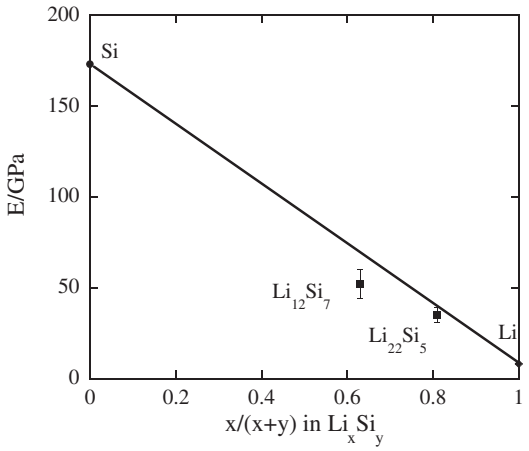

Fig. 2. Young's modulus, E, as a function of atomic fraction of lithium for polycrystalline Li–Si alloys.

0.4%vol. $MoSi_2$ or 0.5%vol. Mo_4O_{11}. Using the Voigt and Reuss models [14] for a mixture of two phases and the Young's modulus for $MoSi_2$ and Mo_4O_{11} and the above volume fractions it was determined that the impurities make less than a 1% contribution to the total modulus hence, the measured value of Young's modulus corresponds to the Young's modulus for the $Li_{12}Si_7$ alloy. Young's modulus for the $Li_{12}Si_7$ alloy is between the measured values for polycrystalline lithium (4.9 GPa from tension [15] or 8.0 GPa from ultrasonic spectroscopy [16]) and polycrystalline silicon (173 GPa from nanoindentation [17]). Fig. 2 shows a plot of Young's moduli for polycrystalline Li–Si alloys as a function of lithium concentration. The solid line connecting Young's modulus for polycrystalline silicon [17] and polycrystalline lithium [16] suggests that Young's modulus linearly decreases with increasing lithium concentration. This result was also observed for predicted values of bulk modulus for amorphous and polycrystalline Li–Si alloys and was attributed to elastic softening with increasing lithium concentration [8,18]. Interestingly, the predicted value of Young's modulus for $Li_{12}Si_7$ (~85 GPa) [8] is significantly greater than the experimentally determined value of Young's modulus for $Li_{12}Si_7$; approximately 1.6 times the measured value. Ratchford et al. [10] previously observed that for $Li_{22}Si_5$, the predicted value of Young's modulus was also significantly higher than the experimentally measured value. Thus, it also appears that for the $Li_{12}Si_7$ alloy that DFT overestimated the value of Young's modulus.

During this study, additional predictions of the bulk moduli for Li–Si alloys using DFT calculations were found [18,19]. Young's moduli were estimated from these predicted values using Eq. (1), where E is Young's modulus, K is bulk modulus, and ν is Poisson's ratio [14]

$$E = 3K(1 - 2\nu) \quad (1)$$

Eq. (1) is based on isotropic behavior, which is a good approximation in this work because $Li_{12}Si_7$ and $Li_{22}Si_5$ alloys are polycrystalline [14]. From Eq. (1), a value for Poisson's ratio is needed. Poisson's ratio for other Li alloys range between 0.2 and 0.4 [10]. Therefore, an average value $\nu = 0.3$ was used to calculate the estimated values of Young's modulus. The estimated values of Young's modulus for $Li_{12}Si_7$ and $Li_{22}Si_5$ are listed in Table 2. Table 2 shows that the estimated values are in excellent agreement with the measured values of Young's modulus listed in Table 1 for $Li_{12}Si_7$ and $Li_{22}Si_5$. From these results, we can conclude the experimental values of Young's modulus for $Li_{12}Si_7$ and $Li_{22}Si_5$ represent the true values for these alloys.

Table 2
Estmated Young's moduli, *E*, from Eq. (1) for $Li_{12}Si_7$ and $Li_{22}Si_5$.

Sample	*E* (GPa)
$Li_{12}Si_7$	52[a]
	60[b]
$Li_{22}Si_5$	38[a]
	42[b]

[a] Ref. [18].
[b] Ref. [19].

4. Conclusion

Polycrystalline $Li_{12}Si_7$ was synthesized. The single-phase purity of the alloy was confirmed by X-ray diffraction, ICP-MS and optical microscopy. Young's modulus for polycrystalline $Li_{12}Si_7$ was determined from nanoindentation testing. The value of Young's modulus was 52.0 ± 8.2 GPa. This value is in excellent agreement with estimated values of Young's modulus calculated from predicted values of bulk modulus using density functional theory.

Acknowledgments

The authors are grateful to the Army Research Laboratory for financial support. This research was performed while JBR held a National Research Council Research Associateship Award at the United States Army Research Laboratory.

References

[1] W.J. Zhang, J. Power Sources 196 (2011) 13–24.
[2] J.M. Tarascon, M. Armand, Nature 414 (2001) 359–367.
[3] C.M. Park, J.H. Kim, H. Kim, H.J. Sohn, Chem. Soc. Rev. 39 (2010) 3115–3141.
[4] U. Kasavajjula, C.S. Wang, A.J. Appleby, J. Power Sources 163 (2007) 1003–1039.
[5] A.S. Arico, P. Bruce, B. Scrosati, J.M. Tarascon, W. Van Schalkwijk, Nat. Mater. 4 (2005) 366–377.
[6] W.-J. Zhang, J. Power Sources 196 (2011) 13–24.
[7] K. Xu, A. von Cresce, J. Mater. Chem. 21 (2011) 9849–9864.
[8] V.B. Shenoy, P. Johari, Y. Qi, J. Power Sources 195 (2010) 6825–6830.
[9] Y.T. Cheng, M.W. Verbrugge, Electrochem. Solid State Lett. 13 (2010) A128–A131.
[10] J.B. Ratchford, B.E. Schuster, B.A. Crawford, C.A. Lundgren, J.L. Allen, J. Wolfenstine, J. Power Sources 196 (2011) 7747–7749.
[11] M. Radovic, E. Lara-Curzio, L. Riester, Mater. Sci. Eng. A: Struct. Mater. Prop. Microstruct. Process 368 (2004) 56–70.
[12] W.C. Oliver, G.M. Pharr, J. Mater. Res. 7 (1992) 1564–1583.
[13] H. Okamoto, J Phase Equilib. Diffus. 30 (2009) 118–119.
[14] C.R. Barrett, W.D. Nix, A.S. Tetelman, The Principles of Engineering Materials, Printice-Hall, Inc., 1973.
[15] P.W. Bridgman, in: Proceedings of the American Academy of Arts and Sciences, vol. 57 (1922), pp. 40–66.
[16] W.M. Robertson, D.J. Montgomery, Phys. Rev. 117 (1960) 440–442.
[17] C.-S. Oh, H.-J. Lee, S.-G. Ko, S.-W. Kim, H.-G. Ahn, Sens. Actuators A: Phys. 117 (2005) 151–158.
[18] H. Kim, C.Y. Chou, J.G. Ekerdt, G.S. Hwang, J. Phys. Chem. C 115 (2011) 2514–2521.
[19] V.L. Chevrier, J.W. Zwanziger, J.R. Dahn, Can. J. Phys. 87 (2009) 625–632.